

Electronic structure of the Cu-O/Ag(110)(2×2)p2mg surface

Daiichiro Sekiba*

INFM, Unità di Genova, Via Dodecaneso33, 16146 Genova, Italy

Daisuke Ogarane and Sachiko Tawara

Institute of Physics, University of Tsukuba, Tennodai 1-1-1, Tsukuba, Ibaraki 305-8571, Japan

Kazutoshi Yagi-Watanabe

Photonics Research Institute, National Institute of Advanced Industrial Science and Technology (AIST), Tsukuba Central 2, Tsukuba 305-8568, Japan

(Received 27 February 2002; revised manuscript received 22 August 2002; published 21 January 2003)

Reviewing the Slater-Koster parameters experimentally collected on various oxygen-adsorbed surfaces, we suggest a scaling law describing the Slater-Koster (SK) parameters between the oxygen and d -electron metals, instead of the conventional Harrison rule. We demonstrate an examination of this scaling law by the comparative study with the angle-resolved ultraviolet photoelectron spectroscopy (ARUPS) measurement on the Cu-O/Ag(110)(2×2)p2mg surface. First, the electronic structure of the Cu-O/Ag(110)(2×2)p2mg surface is determined by ARUPS using synchrotron radiation. The band assignment of O2p and Cu3d is carefully done by means of the cross-section analysis for the 20 and 100 eV photon energy. The obtained electronic structure is interpreted in terms of the tight-binding calculation. In the calculation, we use SK parameters produced by the new scaling law. From the good agreement between the experiment and the calculation, we can see that the scaling law is practically useful.

DOI: 10.1103/PhysRevB.67.035411

PACS number(s): 73.20.At, 73.22.-f, 71.15.-m

I. INTRODUCTION

In the last decades, we have studied the electronic structures of oxygen-adsorbed metal surfaces by means of angle-resolved ultraviolet photoelectron spectroscopy (ARUPS). By interpreting all the experimental results in terms of the tight-binding calculation, we have determined Slater-Koster (SK) parameters of oxygen-metal interaction on the various metal surfaces: Pd(110), Cu(110), Cu(100), Ni(110), Ag(110), and Rh(110).¹⁻⁶ Reviewing these semiempirically determined SK parameters, we noticed that there is a universal scaling law dominating the SK parameters of oxygen-metal interaction. In other words, the SK parameters are determined as the functions of the interatomic distance.

As is well known, this concept to make scaling law of the SK parameters was suggested by Harrison in 1980.⁷ According to this Harrison rule, some of the SK parameters are given as follows,

$$(sp\sigma), (pp\sigma), (pp\pi) = \eta_{ll'm} \frac{\hbar^2}{m} d^{-2},$$

$$(pd\sigma), (pd\pi) = \eta_{ldm} \frac{\hbar^2}{m} d^{-7/2}, \quad (1)$$

where l and l' denote the s or p orbitals, and m indicates the σ or π bondings, respectively. Harrison determined the universal coefficient η by averaging the values obtained on the various systems. While this rule well interprets the generic tendencies of electronic structures of solids, it is not suitable to investigate detailed properties of individual systems. Indeed the SK parameters determined on the oxygen-adsorbed metal surfaces do not obey this rule well. Keeping the simplicity of the Harrison rule, the rule should be given more

practical accuracy optimized to individual cases. From this viewpoint, we suggest a scaling law describing our SK parameters between oxygen and d -electron metals constructed by modifying the Harrison rule.

We introduce a scaling law of the oxygen-metal interaction, and we apply this law to a practical case. As the best candidate for the examination, we picked the Cu-O/Ag(110)(2×2)p2mg surface, where -Cu-O- zigzag chains are formed along the $[1\bar{1}0]$ direction on the Ag(110) surface (see Fig. 1).⁸ This structure is the same as that of the oxygen-adsorbed (0.5-ML) Rh(110) surface.^{9,10}

We report the electronic structure of the Cu-O/Ag(110)(2×2)p2mg surface as the results of ARUPS experiments. Then we make the tight-binding calculation of this surface and compare it with the experimental results. In the calculation, we use the scaling law to determine the SK parameters of Cu-O and Ag-O interactions. We will show the good agreement between the experiment and the tight-binding calculation.

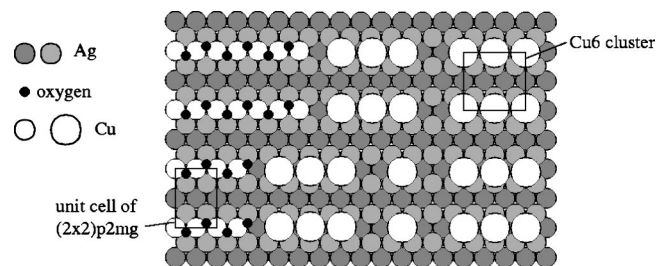


FIG. 1. The surface structure of Cu-O/Ag(110)(2×2)p2mg and Cu₆/Ag(110) surfaces. The open circles indicate Cu atoms, and gray and black circles indicate Ag and oxygen atoms, respectively. This surface structure may be found in Ref. 8.

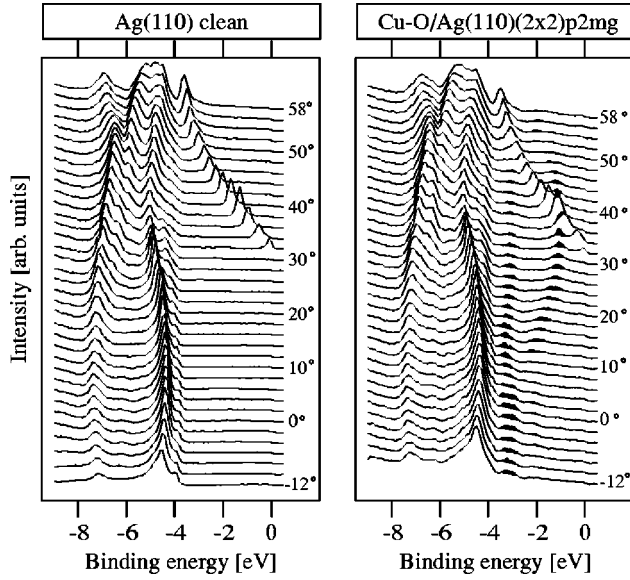


FIG. 2. ARUPS spectra of the clean Ag(110) (left) and Cu-O/Ag(110)(2×2)p2mg (right) surfaces. The spectra were taken along the $[1\bar{1}0]$ direction. The shading indicates the features induced by Cu-O. The p -polarized light of $h\nu=20$ eV photon energy was used. The light incidence angle was $\theta_i=70^\circ$.

II. EXPERIMENT

The substrate sample of Ag(110) was cleaned by Ar^+ -ion bombardment and a 673 K annealing cycle. The Cu-O/Ag(110)(2×2)p2mg surface was prepared by a one-half monolayer of Cu deposition on the oxygen-adsorbed Ag(110)p(2×1)-O surface at room temperature. The (2×2)p2mg structure was confirmed by observation of a sharp low-energy, electron-diffraction (LEED) pattern in which every half order spot ($h/2, 0$) is missing (“ h ” are odd integers, e.g., 1,3,5 . . .). The experiments were made at BL-18A of the Photon Factory, KEK. In the ARUPS measurements, mainly 20 eV p -polarized light was used to detect the photoelectrons coming from both O2p and Cu3d states. To distinguish between O2p and Cu3d states, we made a similar measurement of 100 eV photons and compared the spectra. The light incidence angle was set at 70° from the surface normal and photoelectrons are collected in the light incidence plane in all the measurements. The spectra were collected along the $[1\bar{1}0]$ and $[001]$ directions on the Cu-O/Ag(110)(2×2)p2mg surface.

III. RESULTS

Figure 2 shows the ARUPS spectra of the clean Ag(110) and Cu-O/Ag(110)(2×2)p2mg surfaces along the $[1\bar{1}0]$ direction measured with 20 eV photons. Figure 3 shows the spectra taken along the $[001]$ direction. There are some Cu-O induced features as indicated by shading in the spectra. In the $[1\bar{1}0]$ direction, we can observe a state dispersing from -2 to -1 eV. We also observe a strong and nondispersing feature at -3 eV.

In order to assign origin of these states, we made a cross-

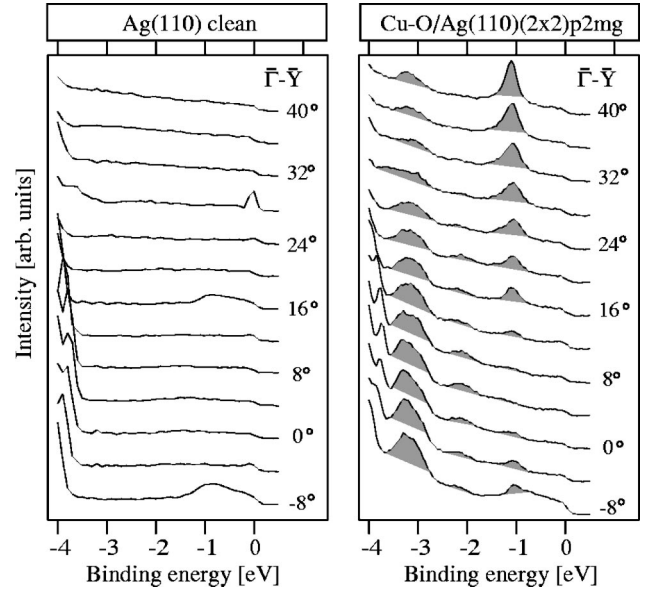


FIG. 3. ARUPS spectra of clean Ag(110) (left) and Cu-O/Ag(110)(2×2)p2mg (right) surfaces. The spectra were taken along the $[001]$ direction. The shading indicates the features induced by Cu-O. The p -polarized light of $h\nu=20$ -eV photon energy was used. The light incidence angle was $\theta_i=70^\circ$.

section analysis. Figure 4 indicates a photon energy dependence of the normal-emission spectra.¹² Relative intensity of the -3 eV peak was enhanced with $h\nu=100$ eV; on the contrary, the -2 eV peak declined or vanished with an increase of photon energy. Comparing photon energy dependence of photoemission cross sections for Ag4d, Cu3d, and O2p orbitals [see Fig. 4(b)], we can ascribe the -2 eV and -3 eV peaks to the O2p and Cu3d states, respectively.

The O2p state which disperses upward from -2 to -1 eV along the $[1\bar{1}0]$ direction (Fig. 2) would be attrib-

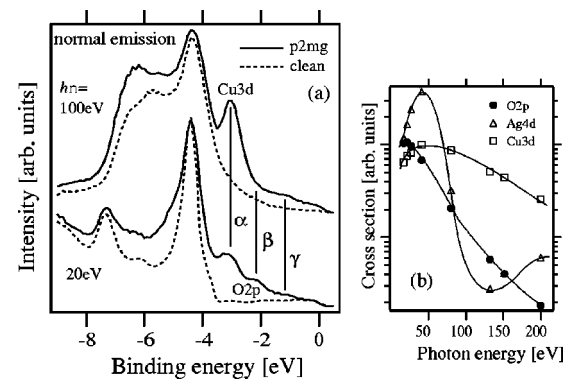


FIG. 4. (a) Normal-emission spectra of clean Ag(110) and Cu-O/Ag(110)(2×2)p2mg surfaces with two types of photon energy, 20 and 100 eV. Solid and dotted lines indicate the spectra of the clean Ag(110) and Cu-O/Ag(110)(2×2)p2mg surfaces, respectively. Three typical features induced by Cu-O are indicated by α , β , and γ . (b) Photoemission cross-section variation with photon energy for the Ag4d, Cu3d, and O2p states (Ref. 12). From this cross-section variation, it is indicated that the state α in (a) is ascribed to the Cu3d, others are assigned to the O2p state.

uted to the antibonding states, as was analyzed from the result on the Ag(110) $p(2\times 1)$ -O surface. This band folds at Γ_{2nd} (corresponds to $\theta_e=32^\circ$) and it shows typical behavior of the $p2mg$ structure.¹³ The Cu3 d peak shows a change in its width and line shape with increasing emission angle and thus we can say this feature should contain several states. Later on we will discuss those O2 p and Cu3 d states in terms of the tight-binding model.

We cannot observe any band dispersion on the spectra along the [001] direction (Fig. 3). This is reasonable because the interactions between the adjacent Cu-O chains along the [001] direction are impossible due to the missing row structure. The electronic structure of the Cu-O chain has one-dimensional behavior.

In Fig. 2, we observed some intensity changes in the Ag4 d bulk band region of $-8\sim 4$ eV and this must include some information about the bonding states. However, it does not seem to be easy to treat the bonding states exactly, as in the case of the Ag(110) $p(2\times 1)$ -O surface.^{5,11} We will not pursue this issue further here since it is quite complicated.

IV. STRUCTURAL MODEL

Before interpreting our experimental results by means of the tight-binding calculations, we need to know the precise structure of the Cu-O/Ag(110)(2×2) $p2mg$ surface including the information on atomic radii. However, no detailed structural analysis of this surface has been done except the suggestion of a structural model based on the scanning-tunneling microscopy images and LEED patterns (see Fig. 1). Therefore we should make an extrapolation for the atomic radii of the adsorbed Cu and O by reviewing many structural analysis reports on other surface alloys.

According to the previous structural analysis on other surface alloys, we find following tendencies of atomic radii of adsorbates. First, the atomic radius of adsorbed metal becomes equal to that of the substrate atom. Second, the adsorbed gaseous atom always keeps almost the same atomic radius, independently of substrates. For example, Cu(100) $c(2\times 2)$ -Pd is a well-known surface alloy, and many tensor LEED structural analyses have been done.¹⁴⁻¹⁶ On this surface the atomic radius of Pd becomes completely the same as that of the substrate Cu. The same phenomenon was pointed out also on the Cu(100) $c(2\times 2)$ -Au surface.¹⁴ Apart from this, we can introduce the bilayer Cu-O film on the Ru(0001) surface, where a Cu-O zigzag chain is formed.¹⁷ On this surface the radius of the Cu atom becomes almost the same as that of the Ru atom, and the radius of the O atom is kept at 0.61 Å. This value of the radius of oxygen is not changed from that on the Ag(110) $p(2\times 1)$ -O surface (0.60 Å).

Thus, also on the Cu-O/Ag(110)(2×2) $p2mg$ surface, we could assume that the radius of the Cu atom is equal to that of the substrate Ag atom, and radius of the O atom is 0.6 Å, like the value on the Ag(110) $p(2\times 1)$ -O surface. In this case, the structural outline of Cu-O/Ag(110)(2×2) $p2mg$ looks like Ag-O/Ag(110)(2×2) $p2mg$ or Ag(110)(2×2) $p2mg$ -O.

V. SLATER-KOSTER PARAMETERS

A. Metal-metal interaction

Here we discuss the SK parameters necessary for our tight-binding calculation. We need three types of SK parameters. The first is the Ag-Ag interaction in the substrate. The second is the interaction of the alloy part, Ag-Cu and Cu-Cu. Finally, the last is the interaction between two different metals (Ag, Cu) and O.

For the Ag-Ag interaction, we adopt the SK parameters determined by Papaconstantopoulos for bulk Ag.¹⁸ These SK parameters of Ag-Ag reproduced well the experimentally determined electronic structures of clean Ag(110) and Ag(110) $p(2\times 1)$ -O surfaces.⁵

For the alloy part (Ag-Cu and Cu-Cu interaction), we prepare the SK parameters by means of the weighted average of the SK parameters for the bulk Ag and Cu, as done in other works.^{19,20} In other words, we simply interpolated the SK parameters of bulk Ag and Cu determined by Papaconstantopoulos as a function of the interatomic distance. We adopt the power-law function $V = \eta \hbar^2 / md^s$, and we fit η and s as the adjustable parameters. Then we substituted the interatomic distance of Ag-Ag for the obtained function. The bulk SK parameters of Ag and Cu determined by Papaconstantopoulos obey well the power law. Therefore the obtained SK parameters by the interpolation are not so different from those of bulk Ag.

B. Oxygen-metal interaction

Here we examine the scaling law describing the SK parameters of oxygen-metal interaction. Figure 5 displays the SK parameters obtained on the various oxygen-adsorbed metal surfaces as the functions of the interatomic distance: Cu(110) (circles), Ni(110) (squares), Ag(110) (triangles), and Rh(110) (crosses).^{2,4-6} As mentioned in the previous study,⁵ these SK parameters seem to obey the following scaling law instead of the Harrison rule of Eq. (1):

$$\begin{aligned} (sP\sigma) &= \eta_{ll'm} \frac{\hbar^2}{m} d^{-2}, \\ (Pp\sigma), (Pp\pi) &= \eta_{ll'm} \frac{\hbar^2}{m} d^{-7/2}, \\ (Pd\sigma), (Pd\pi) &= \eta_{ldm} \frac{\hbar^2}{m} d^{-7/2}, \end{aligned} \quad (2)$$

where P indicates O2 p , and s , p , and d represent the electronic states of metals. The difference from the conventional Harrison rule is the exponents of the $(Pp\sigma)$, $(Pp\pi)$, that is, they are changed from -2 to $-7/2$. While the origin of this change is not clear, we speculate that it is caused by the extremely small electron occupancy of the p -orbital of the d -electron metals. Fitting these scaling laws for the semiempirically obtained SK parameters, we determined η for each SK parameter: $\eta_{sp\sigma}=0.07$, $\eta_{pp\sigma}=0.63$, $\eta_{pp\pi}=0.24$, $\eta_{pd\sigma}=0.33$, and $\eta_{pd\pi}=0.12$. The results of fitting are shown in figures with solid lines. By substituting the expected inter-

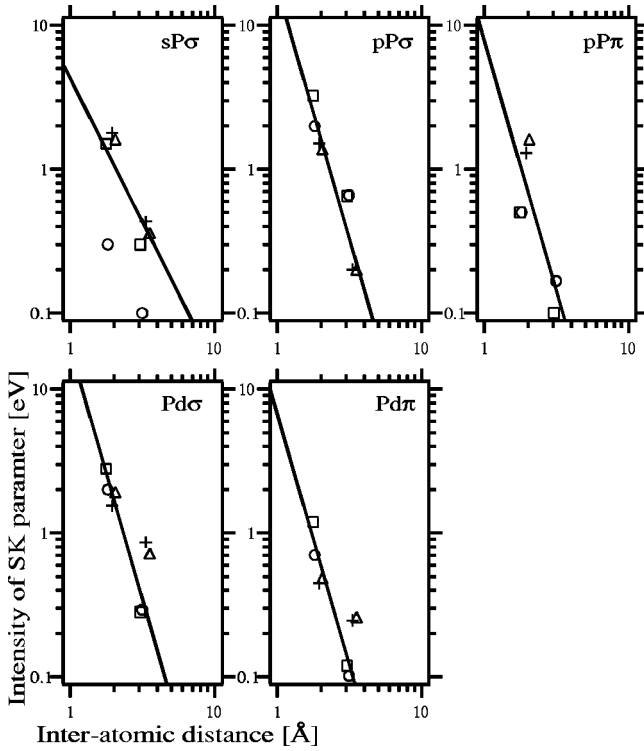


FIG. 5. SK parameters determined on the oxygen-adsorbed Cu(110) (circles), Ni(110) (squares), Ag(110) (triangle), and Rh(110) (crosses) surfaces are plotted in logarithmic scale as the functions of the interatomic distance. The SK parameters were fitted by the scaling law shown in Eq. (3). The results of the fitting are indicated by solid lines in each figure.

atomic distances of oxygen-metal bonding for the scaling law, we can produce the SK parameters for the oxygen-metal interaction.

VI. TIGHT-BINDING CALCULATION

Now we construct the Hamiltonian to make the tight-binding calculation. As a basis set of the Hamiltonian, we considered $O2p$, $Cu3d$, $Cu4s$, $Cu4p$, $Ag4d$, $Ag5s$, and $Ag5p$ orbitals. The first- and second-nearest-neighbor interactions were taken into account. By including ten substrate layers, we diagonalized 384×384 secular equations at 31 k points from the $\bar{\Gamma}$ to the second \bar{X} point. As mentioned above, the SK parameters of the substrate Ag-Ag interaction is referred from the first-principles calculation of bulk Ag. For the alloy part (Ag-Cu, Cu-Cu), the SK parameters are taken by a weighted average of bulk Ag-Ag and bulk Cu-Cu interactions. The SK parameters of oxygen metals are determined by the scaling law. Apart from this, the on-site energies of $Cu3d$, $4s$, $4d$, and $O2p$ are also used as adjustable parameters. The on-site energies of substrate Ag are the same used in the study of $Ag(110)p(2 \times 1)-O$.

Figure 6 shows the comparison of the band structures between the experimental result of ARUPS and the tight-binding calculation. White circles indicate the experimental data, and the gray density plot indicates the result of the tight-binding calculation. The density plot in Fig. 6 repre-

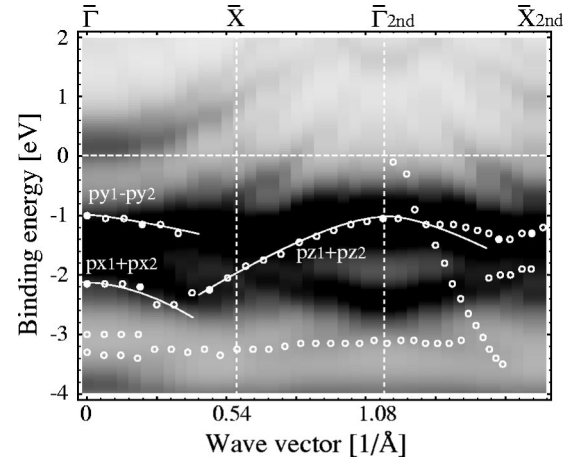


FIG. 6. Comparison of the tight-binding calculation and experiment along $\bar{\Gamma}-\bar{X}$. The density plot indicates the calculation, and open circles indicate the experimental data. Darkness of the density plot indicates intensity of the $O2p$ states ascribed to the Δ_1 representation: px_1+px_2 , py_1-py_2 , and pz_1+pz_2 .

sents the partial densities-of-states (DOS) intensity of the $O2p$ states classified into the Δ_1 representation in terms of the group theory of the $p2mg$ symmetry, i.e., the bands ascribed to px_1+px_2 , py_1-py_2 , and pz_1+pz_2 . We can see that all the $O2p$ bands obtained from the experiment are interpreted by the calculation consistently. The assignment of each oxygen-derived band is indicated in the figure (dotted lines).

The $Cu3d$ band structure is also reproduced by the calculation as can be seen in Fig. 7. The partial DOS of $Cu3d$ states in the Δ_1 representation are indicated as a density plot in the figure: xy_1-xy_2 , yz_1-yz_2 , zx_1+zx_2 , $x^2-y_1^2+x^2-y_2^2$, and $3z^2-r_1^2+3z^2-r_2^2$. It is not simple to discuss the agreement between the experiment and calculation of $Cu3d$ states, be-

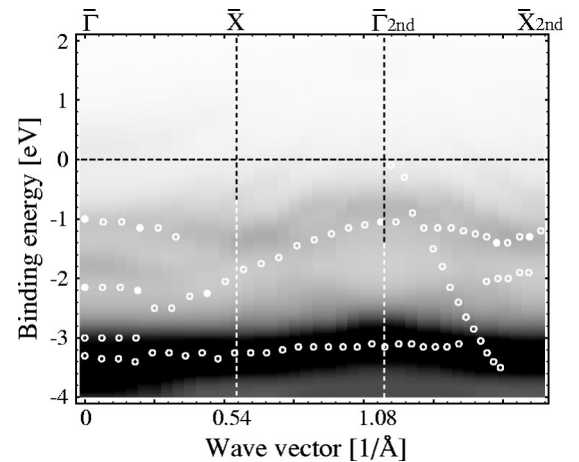


FIG. 7. Comparison of the tight-binding calculation and experiment along $\bar{\Gamma}-\bar{X}$. The density plot indicates the calculation, and open circles indicate the experimental data. Darkness of the density plot indicates intensity of the $Cu3d$ states ascribed to the Δ_1 representation: xy_1-xy_2 , yz_1-yz_2 , zx_1+zx_2 , $x^2-y_1^2+x^2-y_2^2$, and $3z^2-r_1^2+3z^2-r_2^2$.

TABLE I. The on-site energies of Cu3*d*, 4*s*, and 4*p* are shown and are compared with those determined on the Cu(110)*p*(2×1)-O surface. The notation Cu3*d*₁ and Cu3*d*₂ represents the on-site energies of *xy*, *yz*, *zx*, and *x*²-*y*², 3*z*²-*r*², respectively. The on-site energies of Ag are also displayed for the comparison.

On site	Cu(110) <i>p</i> (2×1)-O	Ag(110) <i>p</i> (2×1)-O	Cu-O/Ag(110)(2×2) <i>p</i> 2 <i>mg</i>
O2 <i>p</i>	-3.9	-2.0	-2.0
Cu4 <i>s</i>	2.91		
4 <i>p</i>	10.52		-0.5 eV from
3 <i>d</i> ₁	-2.82		Cu(110) <i>p</i> (2×1)-O
3 <i>d</i> ₂	-2.84		
Ag5 <i>s</i>		2.32	
5 <i>p</i>		8.46	same as
4 <i>d</i> ₁		-5.30	Ag(110) <i>p</i> (2×1)-O
4 <i>d</i> ₂		-5.53	

cause there are five different states in a same energy region. However, we can see that the main peak of Cu3*d* states in the experiment slightly disperses upward from $\bar{\Gamma}_{1st}$ to $\bar{\Gamma}_{2nd}$. This small dispersion is well reproduced by the most intense part of the tight-binding calculation.

Thus the SK parameters produced by the scaling law well described the electronic structure of the Cu-O/Ag(110)(2×2)*p*2*mg*. We roughly define the agreement between the experiment and the calculation by the averaged deviation on some points of the electronic bands as follows:

$$I = \frac{1}{n} \sum_{i=1}^n |E_i^{exp} - E_i^{cal}|. \quad (3)$$

We chose eight typical points from the experimentally determined energy states to compare them with the calculations, and those are indicated by filled circles in Fig. 6. When we use the scaling law, the agreement was $I_{scaling} = 0.186$ (eV). On the other hand, in the cases in which we use the SK parameters obtained on Cu(110)*p*(2×1)-O (Ref. 2) and Ag(110)*p*(2×1)-O,⁵ the calculations show less agreement, $I_{Cu} = 0.332$ and $I_{Ag} = 0.248$, respectively. The result of the best fitting was $I_{best} = 0.124$. The scaling law gives much better agreement than the SK parameters of Ag(110)*p*(2×1)-O, even though the oxygen-metal interatomic distances of Cu-O/Ag(110)(2×2)*p*2*mg* are almost equal to those of Ag(110)*p*(2×1)-O. This implies that the scaling law includes the property not only of the Ag-O interaction, but also of the Cu-O interaction, providing a good description of the electronic structure of the surface alloy.

Finally we mention the on-site energies of O2*p*, Cu3*d*, 4*s*, and 4*p*, which were used as the fitting parameters. In Table I, the obtained on-site energies are displayed and are

compared with the on-site energies of Ag and Cu on the Cu(110)*p*(2×1)-O surface. In the studies of Cu(110)*p*(2×1)-O (Ref. 2) and Ag(110)*p*(2×1)-O,⁵ the on-site energies of Cu and Ag were taken from the values determined by Papaconstantopoulos for the bulk Cu and Ag. The offset for those on-site energies was determined to reproduce the experimental band structures of clean Cu(110) and Ag(110). In the present calculation, in principle, we used the same on-site energies for the substrate Ag and adsorbed Cu. However, we needed to add a -0.5 eV surface shift for the on-site energies of Cu. So far this surface shift still calls for an interpretation.

VII. CONCLUSION

Reviewing the SK parameters collected on the oxygen-adsorbed Cu(110), Ni(110), Ag(110), and Rh(110) surfaces, we suggest the scaling law dominating the SK parameters of oxygen- and *d*-electron metal interaction. We interpreted the electronic structure obtained via an ARUPS experiment on the Cu-O/Ag(110)(2×2)*p*2*mg* surface by means of the synchrotron radiation with 20 and 100 eV photon energies, and we interpreted the electronic structure by means of the tight-binding calculation and the new scaling law. The SK parameters produced by the scaling law well reproduced the experimentally determined electronic structure.

ACKNOWLEDGMENTS

We are grateful to the late Professor Hirohito Fukutani, who offered thoughtful and helpful comments during this work. We would like to thank T. Kinoshita, T. Okuda, and A. Harasawa for collaboration and discussions during the experiment.

*Email address: sekiba@fisica.unige.it

¹K. Yagi, K. Higashiyama, and H. Fukutani, Surf. Sci. **295**, 230 (1993).

²R. Ozawa, A. Yamane, K. Morikawa, M. Ohwada, K. Suzuki, and H. Fukutani, Surf. Sci. **346**, 237 (1996).

³D. Sekiba, T. Inokuchi, Y. Wakimoto, K. Yagi-Watanabe, and H. Fukutani, Surf. Sci. **470**, 43 (2000).

⁴H. Fukutani, K. Suzuki, A. Yamane, R. Ozawa, Y. Gunji, and K. Higashiyama, Surf. Sci. **365**, 248 (1996).

⁵D. Sekiba, H. Nakamizo, R. Ozawa, Y. Gunji, and H. Fukutani, Surf. Sci. **449**, 111 (2000).

⁶The ARUPS experiment (at BL-18A of the Photon Factory, KEK) and tight-binding calculation were done on the Rh(110)(2×2)*p*2*mg*-O surface. The results will be submitted to Surface

- Science. Contact the corresponding author.
- ⁷W.A. Harrison, *Electronic Structure and the Properties of Solids, The Physics of the Chemical Bond* (Freeman, San Francisco, 1980).
- ⁸Y. Matsumoto and K. Tanaka, *Surf. Sci. Lett.* **350**, L227 (1996).
- ⁹M. Gierer, H. Over, G. Ertl, H. Wohlgemuth, E. Schwarz, and K. Christmann, *Surf. Sci. Lett.* **297**, L73 (1993).
- ¹⁰G. Comelli, V.R. Dhanak, M. Kiskinova, N. Pangher, G. Paolucci, K.C. Prince, and R. Rosei, *Surf. Sci.* **260**, 7 (1992).
- ¹¹L.H. Tjeng, M.B.J. Meinders, and G.A. Sawatzky, *Surf. Sci.* **236**, 341 (1990).
- ¹²J.J. Yeh and I. Lindau, *At. Data Nucl. Data Tables* **32**, 1 (1985).
- ¹³K.C. Prince, *J. Electron Spectrosc. Relat. Phenom.* **42**, 217 (1987).
- ¹⁴S.C. Wu, S.H. Lu, Z.Q. Wang, C.K.C. Lok, J. Quinn, Y.S. Li, D. Tian, F. Jona, and P.M. Marcus, *Phys. Rev. B* **38**, 5363 (1988).
- ¹⁵T.D. Pope, M. Vos, H.T. Tang, K. Griffiths, I.V. Mitchell, P.R. Norton, W. Liu, Y.S. Li, K.A.R. Mitchell, Z.-J. Tian, and J.E. Black, *Surf. Sci.* **337**, 79 (1995).
- ¹⁶C.J. Barnes, E. AlShamaileh, T. Pitkanen, P. Kaukasoina, and M. Lindroos, *Surf. Sci.* **492**, 55 (2001).
- ¹⁷Ch. Ammer, K. Meinel, A. Beckmann, H. Neddermeyer, and K. Heinz, *Surf. Sci.* **482-485**, 1298 (2001).
- ¹⁸D.A. Papaconstantopoulos, *Handbook of The Structure of Elemental Solids* (Plenum, New York, 1986).
- ¹⁹P.M. Laufer and D.A. Papaconstantopoulos, *Phys. Rev. B* **35**, 9019 (1987).
- ²⁰J. Tersoff and L.M. Falicov, *Phys. Rev. B* **24**, 754 (1981).